PHYSICAL REVIEW B **70**, 045413 (2004)

Ab initio total energy study of ZnO adsorption on a sapphire (0001) surface

Yang Chun
Institute of Microelectronics and Solid State Electronics,
University of Electronic Science and Technology of China, Chengdu 610054, China
and Institute of Mathematics and Software Science, Sichuan Normal University, Chengdu 610068, China

Li Yan-rong
Institute of Mcroelectronics and Solid State Electronics, University of Electronic Science and Technology of China,
Chengdu 610054, China

Li Jin-shan
Institute of Chemical Materials, China Academy of Engineering Physics, Mianyang 621000, China

(Received 30 December 2003; published 20 July 2004)

The sapphire (0001) surface and the adsorption of ZnO are theoretically calculated by using a plane wave ultrasoft pseudo-potential method based on density functional theory. By comparing the PDOS of the Al and the O before and after the surface relaxation, we demonstrate different sapphire (0001) surface states, and changes in surface chemical bonding resulting from Al and O are analyzed. The bonding processing of a ZnO molecule on the surface of Al_2O_3, adsorption energy and bonding orientation, and change in surface structure as well as the characters of surface chemical bonding are further investigated. We conclude that the surface inward relaxation in the first layer Al-O is weakened, even eliminated after the surface adsorption of the ZnO; chemical bonding energy achieved 4.4 ± 0.4 eV. There is a deflected angle of 30° between the chemical bonding of the ZnO (0.185 ± 0.01 nm) and the adjacent surface Al-O bonding; the stable chemical adsorption site of Zn is just about 30° deflected from the O-hexagonal symmetry of the α-$Al_2O_3(0001)$ surface. Through analysis of the atomic populations, density of state, and bonding electronic density before and after the adsorption, it is revealed that the chemical bonding formed by the O^{2-} of the ZnO and the surface Al^{3+} is characterized by strong ionic bonding, while the bond of the Zn^{2+} and the surface O^{2-} has a covalent character, which mainly comes from the hybridization of the Zn 4s and the O 2p and partially from the hybridization of the Zn 3d and the O 2p, so as to facilitate the forming of tetrahedral coordination in the initial stage of the ZnO films growth. Hence it is favorable for the formation of the wurtzite structure.

DOI: 10.1103/PhysRevB.70.045413 PACS number(s): 68.43.Bc, 68.35.Bs, 73.20.−r, 71.15.−m

I. INTRODUCTION

The sapphire (α-Al_2O_3) is widely applied for the substrates of electronic thin films semiconductor material, such as ZnO, AlN, and so on. The ZnO thin films developed from sapphire substrates has an application prospect in photoelectric and semiconductor laser components.[1] The ZnO thin films deposited on sapphire (0001) through pulse laser deposition (PLD) and molecule beam epitaxy (MBE) technology are of high quality. There are many experimental reports on the preparing method, growing characters, and morphology about the ZnO thin films growth on the α-$Al_2O_3(0001)$ substrate;[2–6] but there is no theoretical calculation on the initial growing mechanism of the ZnO thin films deposited on the α-$Al_2O_3(0001)$ surface.

In the growing process of thin-film material by MBE, the surface structure and defects of substrates have a significant impact on the morphology and pattern as well as interface behavior of film growth. As a result it has a decisive effect on the function of thin-film material. In addition, the adhesion, diffusivity, and bonding of particles on substrates during deposition are essential to the initial growing characters of nucleation during thin films' growth. No sufficient studies and experiments are available on the surface atomic structure, surface bonding and surface charge, surface adsorption, or surface potential energy, especially on complex oxidized surfaces.[7,8] Therefore, to calculate the surface of crystal as well as chemical and physical adsorption by use of reliable theories has become an important method to the study of crystal surface.

As we know the diffusion of the ZnO on the α-$Al_2O_3(0001)$ surface, adsorption site, adhesion, and bonding crucially link to the further forming of the island of ZnO particle cluster so as to have a critical impact on the growing of the ZnO thin films. Therefore, to investigate the adsorption process and the bonding character of the ZnO on the substrate's surface is of great significance in terms of the initial growing mechanism of the ZnO thin films heteroepitaxy. It is evident that the adsorption of the ZnO is dependent primarily upon the atomic structure and electronic states of the α-$Al_2O_3(0001)$ surface. Hence, initially it is necessary for us to create a relaxed α-$Al_2O_3(0001)$ surface to analyze surface atomic and electronic structure. Later, the adsorption model of ZnO on the surface is configured.

A number of references have already calculated the surface atomic structure of the α-$Al_2O_3(0001)$[9–16] and its electronic structure.[14–16] Many consistent results with regard to the calculation of the α-$Al_2O_3(0001)$ surface relaxing have been reported. But for the calculation of its electronic structure, Godin and LáFemina[14] computed the energy band and surface state after the relaxation of the surface $1\times1(0001)$ and concluded that the surface atom Al-O is rehybridized to sp^2 bonding by analyzing topological structure. V. E. Puchin *et al.*[15] pointed out that surface relaxation has a strong impact on DOS through measuring the density of surface state with the adoption of UV photoelectron spectroscopy (UPS) and metastable impact electron spectra (MIES); but no further analysis has been done. Wander, Searle, and Harrison[12] presented the DOS map calculated by HF+LYP and suggested that the valence bond of the α-$Al_2O_3(0001)$ is of an O 2p character. However, the relationship between the surface relaxing and the surface states of the α-$Al_2O_3(0001)$ have not been more extensively discussed. So it is necessary to further study the fields mentioned above.

Although our calculated results of various slab (2×2) models for the α-$Al_2O_3(0001)$ surface are consistent with these reports.[11–13] More importantly, when compared with the electronic structure changes before and after surface relaxation, the results supplement the description of Wander, Searle, and Harrison;[12] Godin and LáFemina;[14] and Puchin *et al.*[15] on the α-$Al_2O_3(0001)$ surface electronic state. Relative content will be described in Sec. III A. The major purpose of this paper is to study the surface adsorption of the ZnO molecule on the α-$Al_2O_3(0001)$, which is arranged as follows. Following a brief introduction on the basic calculation method in Sec. II. Section III illustrates and discusses the results in detail, including: (a) the α-$Al_2O_3(0001)$ surface, (b) the ZnO adsorption process and surface structure, (c) analysis on Mulliken population, (d) bonding and density of state, and (e) electron local function (ELF). Finally, a summary is presented in Sec. IV.

II. METHODOLOGY

The calculations are based on density functional theory (DFT) in the general gradient approximation (GGA PW91) proposed by Perdew *et al.*[17] and employ Vanderbilt ultrasoft pseudo-potentials (USP).[18] Electron wave functions are expanded in terms of a plane wave basis set, and electronic ground state is reached using a conjugate gradients minimization as implemented by the computer code CASTEP.[19,20] The USP, which are available with CASTEP, define the number of valence electrons that are treated explicitly in the calculation and for O $2s^22p^4$, Al $3s^23p^1$, and Zn $3d^{10}4s^2$ states. Under density function theory, the calculation parameters are not sensitive to bonding length and geometric structure in comparison with the calculation of bonding energy. The charge density distribution has very small changes, as small as a quadratic mean deviation in the magnitude of 10^{-4} in calculation conditions, which are especially insensitive to numerical integration points.[21,22] That is, a kinetic energy cutoff E_{cut} of 340 eV for the electrons is used because it could be appropriately reduced through USP based on DFT. For k-point sampling, we have actually employed a symmetrized $3\times3\times2$ Monkhorst-Pack mesh in Brillouin zone with18 k-points for optimizing[23] the α-$Al_2O_3(0001)$ 2×2 surface and $5\times2\times1$ with 10 k-points for dynamic calculating. The time step for the solution to dynamic KS equation (with the accuracy of 5.0×10^{-6} eV/atom) is configured as 1.0 fs. The total simulation time is 1.5 ps, and the system temperature is constant at 400° C.

Through the structure optimization and the calculation of relaxation in the α-$Al_2O_3(0001)$ surface and the calculations on the bond length and bond energy of the ZnO molecule, the results conform to those of Refs. 24 and 25 satisfactorily. The bond length of the ZnO is also quite consistent with the result calculated by Gauss98 software package (0.171 nm), which testifies that our results are reliable. Besides, the Projection scheme[26] is used to convert electronic plane waves into a localized basis, and the principle of Mulliken[27] is used for the analysis of the electronic distribution outside the nucleus.

III. RESULT AND DISCUSSION

A. α-$Al_2O_3(0001)$ surface

A slab model of super-lattice (2×2) is constructed by 10 atoms with literature values[28,9] $(a=0.5128,\ \phi=55°20')$;[28,9] optimization is made to the parameters of lattice with the error of the resulting crystal parameter ($a_0=0.482$ nm) less than 1.3% compared with experimental value (0.476 nm).[29] The calculated result in the distance of surface relaxation is consistent with the reference results mentioned in the introduction. Different models with different terminating atomic layers 6, 9, 12, 15, 18 of the α-$Al_2O_3(0001)$ surfaces are constructed. First, we calculate the surface structure of the α-$Al_2O_3(0001)$ in view of energy, and then we prove that the most outside single-layer Al is the most stabilized surface structure. In the case of multiple layers (over 4 layers) relaxation, larger relaxations mainly occur at layers 6, 9, 12, 15, 18 of the surface Al atoms. The relaxed distance from the most outside Al-layer to the second O-layer of the α-$Al_2O_3(0001)$ is 0.0980 nm, 0.0918 nm, 0.0796 nm, 0.0801 nm, and 0.0792 nm, respectively, which indicates that the thickness of the calculated slab model has an effect on the calculation results of the relaxation. In the case of more than 12 layers, the long-range effect of more internal atoms on the surface is closer to actual bulk. The relaxed distance from the outmost surface Al-layer toward inside is 0.079 ± 0.01 nm, which complies with the error range of Baxter *et al.*;[11] Wander, Searle, and Harrison;[12] Gomes *et al.*[13] (±0.01 nm). In another aspect, the Pauli repulsion becomes smaller if the chosen parameter E_{cut} is relatively small in the calculation of the thin slab, which leads to the relaxation being lager in DFT calculation. After the surface relaxing, as the radius of O^{2-} (0.132 nm), it is much larger than the radius of Al^{3+} (0.051 nm); actually the O atoms will be exposed on the outmost surface of the α-$Al_2O_3(0001)$. Inward relaxing means that the interaction between the aluminium ions of nominal charge Al^{3+} is screened by the second-layer oxygen ions. There are obvious changes in the bonding length of surface Al-O before and after relaxing, and the length after relaxing (0.170 nm) is obviously decreased $(-9.0\pm0.2\%)$ form what it was before (0.186 nm), which is very close to the calculation value of

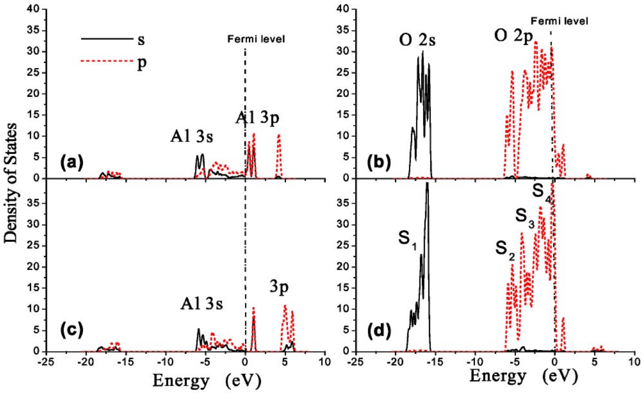

FIG. 1. (Color online) Description of the PDOS for the surface atoms. Where (a) and (c) are the PDOS of the Al before and after relaxation, respectively, and (b) and (d) are the PDOS of the O before and after relaxing, respectively.

Godin and LáFemina[14] and Wander, Searle, and Harrison[12] (−8.9%).

Much research has been done on the geometrical structure of the α-$Al_2O_3(0001)$ surface. However, the surface electronic structures play a significant role in the surface adsorption as well as the growing of thin films. It is necessary to have a further discussion on the action of surface relaxing on the changes of the surface electronic states.

Figures 1(a) and 1(c) illustrate the partial density of states (PDOS) of the surface Al-layer before and after relaxing, respectively. Ofter the relaxation of the surface, the 3p orbitals of Al will be further split, and the lowest empty surface state will mainly be $3p_z$ of Al located around 4.5 eV above the Fermi level, with some overlapping of Al 3s and O 2p in it, which is consistent with the conclusion of Wang, Chaka, and Scheffler[30] (4.5 eV).

Figures 1(a) and 1(c) display the PDOS of the surface O-layer before and after relaxing, respectively. As a result of the observation of changes in the PDOS, splitting occurs obviously in S_1, S_2, S_3, and S_4, with S_1 from the 2s-occupied state of O located between $-15.6 \sim -18.5$ eV, and S_2, S_3, and S_4 from the occupied state of 2p orbits of O located between $-6.0 \sim 0.0$ eV. S_2, S_3, and S_4 just overlap with 3s of surface layer Al, and hence form the hybridization of sp^2, and accordingly, the suggestion proposed by Godin and LáFemina[14] and Wang, Chaka, and Scheffler[30] on the sp^2 hybridization of the surface Al-O has been further proved. However, the Al-O bonds on the clean α-$Al_2O_3(0001)$ surface have more of the character of a strong ionic bond. The relaxing causes the redistribution of a large quantity of surface O^{2-} charge, which manifests the surface obviously in the surface state of the O atoms, and is sure to produce an even lower surface energy. Our calculation of the surface energy is $1.60\ \mathrm{J/m^2}$, which is very close to the literature value by Siegel, Hector, and Adams[31] ($1.59\ \mathrm{J/m^2}$).

Since the O atom layer exposes on the outermost surface of the α-$Al_2O_3(0001)$ after relaxing, the surface obviously shows the O-surface state, and thus the outmost surface O atoms possess with a larger amount of negative charge, which is favorable for the combination of Zn^{2+} with O^{2-} of the surface. In view of the bonding energy of the Zn-O and the Al-O bond, the Al-O bonding energy (512.1 kJ/mol) is much higher than that of the Zn-O (284.1 kJ/mol),[24] therefore, the O^{2-} in the ZnO molecule should be easy to combine with the Al atoms on the substrates. Well then, which is the first to combine with the α-$Al_2O_3(0001)$ surface, the Zn or the O of the ZnO? The position of the ZnO on the surface adsorption and bonding action is closely related to the further forming the island of the ZnO cluster, thus exerting an impact on the growth of thin films. All of these require further theoretical research.

B. Adsorption process and surface structure

For the two adsorption models of the ZnO, the substrates are adopted with an optimized super-lattice slab surface (2×1) model with 6 atomic layers and the surface structure with surface terminating atom in Al-single-layer. In this paper, a lot of attention has been given to the position of surface adsorption, structure of adsorption molecule, and the orientation of space falling, except environmental impact on the substrate's surface. In order to observe the combining sequence of the Zn and the O of the ZnO molecule with the Al and the O of the α-$Al_2O_3(0001)$ surface, we place an optimizing gaseous ZnO molecule (bond length: 0.167 nm) horizontally onto the top with a distance of 0.30 nm from the α-$Al_2O_3(0001)$. Enough consideration has been given to the impact of short vacuum height, which is set as 2.0 nm, as illustrated in Fig. 2(a). For convenient description, the O of the ZnO molecule, which combine with surface Al is expressed as (Zn)O-Al, and that of the Zn with the surface O of the α-Al_2O_3 substrates is marked Zn-O(substrate).

The surface atomic structure of the α-$Al_2O_3(0001)$ substrates is O-hexagonal symmetrical. In order to investigate major adsorption locations on the surface, we set 8 different major adsorption sites on the basis of observing the symmetrical structure of the 2×2 surface atoms. These locations can be considered as the initial growing sites of the ZnO thin films [see Fig. 2(b)]. In the adsorption model of 2×1, we only consider two cases of the ZnO molecule falling horizontally. One is model A, where the Zn and the O is located at the top of adsorption site S7 and S6, respectively, as are shown in Fig. 2(c). The distance of the Zn of the ZnO molecule from the 2 Al positions (Al1 and Al2) is equal, and the O is close to the Al2 position, while the distance from the O of the ZnO to the Al1 and Al2 of the surface is equal in model B, and the Zn is close to the Al2 position displayed in Fig. 2(d). Both models A and B are employed with the same substrate structure whose bottom atomic layers are fixed, and with the same calculation conditions, which are used to observe the effects of the distance between Zn or O and the Al on the surface adsorption.

The adsorption process of model A dislayed in Fig. 3 and 4, A①～④ can be divided into 4 stages: ① $0 \sim 0.08$ ps is the physical process. The Zn of the ZnO molecule is adsorbed down initially and is about 0.03 nm lower than the O. It is mainly of the action of static electricity between the Zn^{2+} and the O^{2-} on the α-$Al_2O_3(0001)$ surface. During the process, the distance of the O of the ZnO molecule from the Al2 position is $0.289 \sim 0.251$ nm. The Zn is located at the top of

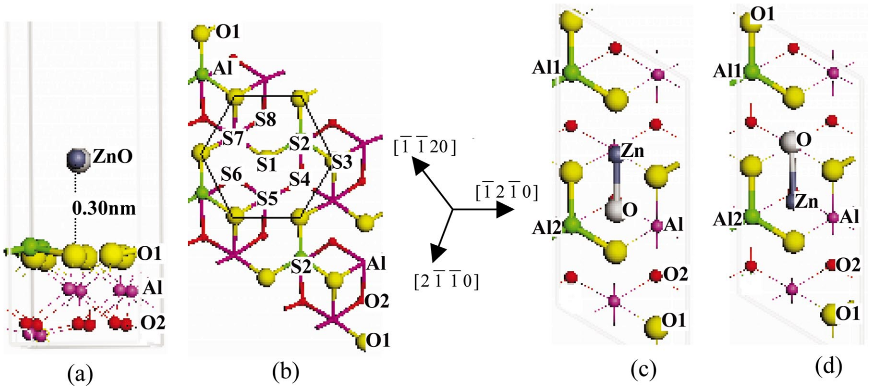

FIG. 2. (Color) The α-$Al_2O_3(0001)$ surface adsorption sites and the ZnO adsorption models: (a) ZnO adsorption slab model, (b) different adsorption sites on the top layer, (c) adsorption model A, and (d) adsorption model B. Red balls in the figure represent bottom O atoms in the substrates, which are marked O2; purple balls represent bottom Al atoms; the bigger green balls represent the 2 Al atoms of the surface, and are marked as Al1 and Al2, respectively; the biggest yellow balls represent the O atoms on the substrates, and are marked as O1. The deep gray balls represent Zn atoms, and the light gray and bigger balls represent the O atoms of the ZnO molecule.

S7 in a distance about 0.286～0.245 nm from the surface. The O of the ZnO molecule slightly shifts in the direction of $[1\bar{2}10]$, where the physical adsorption energy is about 0.24 eV. ② 0.08～0.10 ps is the bonding process of (Zn)O-Al. The O of the ZnO molecule continuously shifts in the direction of $[1\bar{2}10]$ and approaches Al2 at the substrates swiftly. It starts (Zn)O-Al2 bonding at 0.09 ps, whose length is 0.192 nm. While at 0.10 ps, strong (Zn)O-Al2 chemical bond is formed, whose length is 0.161 nm. The Zn of the (Zn)O-Al2 bond is located at the top of S7 in a distance of 0.230 nm from the surface, and the adsorption energy achieves 2.3 eV. ③ 0.10～0.15 ps is the bonding process of Zn-O (substrate). The bonding length of (Zn)O-Al2 is oscillated between 0.168～0.195 nm. The Zn combines with the O of the substrates swiftly and moves toward site S6 slightly. The distance of Zn-O(substrates) is about 0.171 nm. ④ After 0.15 ps, the ZnO molecule, together with the surface of substrates, slowly forms a stable adsorption state. At the lowest system energy (0.78 ps), the adsorption energy of the ZnO molecule at the α-$Al_2O_3(0001)$ surface is about 4.4±0.4 eV, and the adsorption position of the Zn is close to S7 [see Fig. 4, A-④].

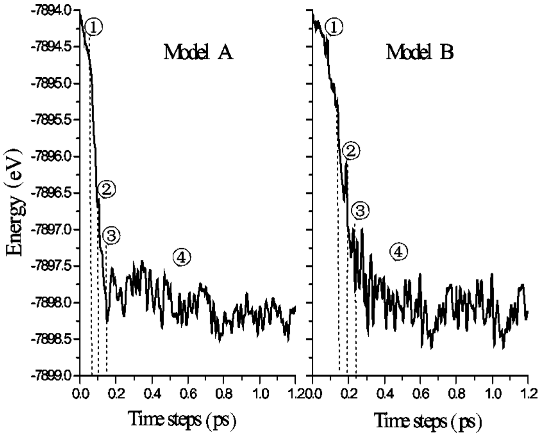

FIG. 3. The ZnO adsorption process and the changes in system energies.

Similar to model A, the process is also divided into 4 stages as are shown in Fig. 3 and Fig. 4 B-①～④: ① 0～0.15 ps is the physical process. The ZnO molecule moves toward $[10\bar{1}0]$ initially, where the Zn is adsorbed downward with a distance of 0.28 nm from the surface. At 0.08 ps, it starts to rotate toward $[1\bar{2}10]$; the O of the ZnO molecule approaches Al2, and the Zn moves toward the site S5. ② 0.16～0.19 ps is the bonding process of (Zn)O-Al. Similar to that of model A, the chemical bond length of O-Al2 at 0.19 ps is 0.159 nm, where Zn is located at the adsorption site between S5 and S6 in a distance about 0.226 nm from the surface. ③ 0.19～0.24 ps is the bonding process of Zn-O(substrate). (Zn)O-Al2 maintains a bonding state, and the Zn combines with the O on the α-$Al_2O_3(0001)$ surface swiftly, where is located at between S5 and S6 at 0.180 nm from the surface. ④ After 0.24 ps, following the adjustment in the bonding length and angle of (Zn)O-Al or Zn-O(substrate), system energy is fallen and stabilized gradually. At the lowest place of system energy (0.67 ps), the adsorption energy of the ZnO molecule at the α-$Al_2O_3(0001)$ surface is 4.4±0.4 eV, and the adsorption position of the Zn is close to S5 [see Fig. 4, B-④].

A comparative analysis of the adsorption process of models A and B indicates that the O and Zn bonded with the adjacent surface Al and O, respectively, in the same way as in model A even though the O of the ZnO molecule in model B is far from Al2 at the α-$Al_2O_3(0001)$ surface and has had a longer physical movement and adsorption. At the stabilized adsorption site, the bonding length of (Zn)O-Al is 0.182 with amplitude of 0.011 nm. The bond length of the ZnO after adsorption is 0.185, and the amplitude is ±0.010 nm. The bond length and adsorption energy after adsorption imply that the ZnO has had a strong chemical adsorption at the α-$Al_2O_3(0001)$ surface. The Zn at stabilized adsorption sites S5 and S7 just has a 30° deflexion away from the surface O-hexagonal symmetry. It can be seen from A-④ in Fig. 4 that the ZnO after adsorption is parallel with $[\bar{2}110]$, and there is a 30° deflexion angle from a Al-O bond (at $[\bar{1}010]$ direction) of the surface Al2. For model B, the ZnO$[\bar{1}2\bar{1}0]$

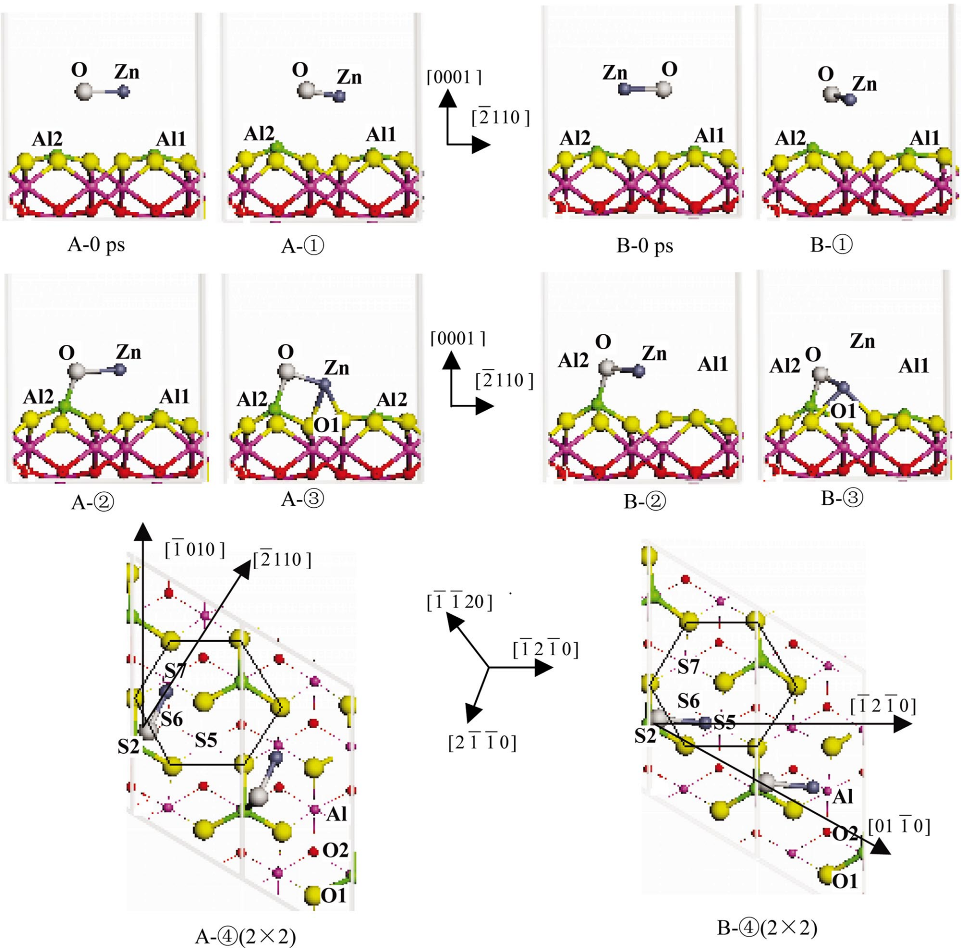

FIG. 4. (Color) The trajectories for the 4 stages of the ZnO adsorption process: ① Physical adsorption, ② (Zn)O-Al bonding, ③ Zn-O(substrate) bonding, and ④ Stabilized adsorption site. Red balls in the figure represent bottom O atoms at substrates, purple balls bottom Al atoms, green balls surface Al atoms, yellow balls surface O, and deep gray and light gray balls ZnO molecules.

after adsorption also has a 30° deflexion angle from another Al-O bonding (at $[01\bar{1}0]$ direction) of the surface Al2 see B-④ in Fig. 4.

Despite both the ZnO films deposited on the (0001) sapphire by laser molecular beam epitaxy (L-MBE), by plasma-assisted molecular beam epitaxy (P-MBE)[2] techniques, or by pulsed-laser deposition (PLD),[3–6] the films are characterized by an expected six-fold symmetry of an epitaxial hexagonal layer. This in-plane orientation relationship corresponds to a 30° rotation of the ZnO unit cell with respect to the unit cell of sapphire.

From the experiment of the researcher Yefan *et al.*,[2] the RHEED indicates an initial incommensurate growth of ZnO on Al_2O_3 in a two-dimensional (2D) nucleation mode. The $[2\bar{1}\bar{1}0]$ orientation of ZnO aligns with the $[1\bar{1}00]$ direction of Al_2O_3, which leads to 30° rotation of the crystal orientation of the ZnO epilayer against the Al_2O_3 substrates. Fons *et al.*[3] and Millon *et al.*[4] reported that the ZnO films were c-oriented and that a 30° rotation in the basal plane occurred such that the ZnO $[1\bar{1}00]$ direction was aligned to the sapphire $[1\bar{2}10]$ direction by x-ray pole figure measurements. Ohkubo *et al.*[5,6] observed that the ZnO films on atomically flat substrates showed two in-plane orientations, ZnO $[10\bar{1}0] \parallel$ sapphire $[10\bar{1}0]$ and ZnO $[10\bar{1}0] \parallel$ sapphire $[11\bar{2}0]$, rotated by 30° for films that grew at low (400–450 °C) and high (800–835 °C) temperatures, respectively. After discussion of these reasons, all experimental reports conclude the ZnO lattice aligns itself with the oxygen sublattice in Al_2O_3, and thus, the lattice mismatch is reduced from around 32% to 18%. There are no further theoretical explorations.

In a film's heteroepitaxial growth, the actual film orientation is determined at the initial stage of the epitaxy; the atomic structure of the substrates surface and the surface dynamics of the precursors on the substrates can be expected to play a major role in the final in-plane film orientation. The initial adsorption of the ZnO on the α-$Al_2O_3(0001)$ would determine the nucleation and following formation of the ZnO films. The results of our adsorption models of ZnO(Model A and Model B) reveal that Zn at the surface stabilized adsorption sites just has a 30° deflexion on the O-hexagonal symmetry of the α-$Al_2O_3(0001)$. We demonstrate that the strong chemical adsorption sites are located at places about 30° apart from the O at the substrates when the (Zn)O-Al bonding is produced, where the strongest Zn-O bond is formed. In terms of micromechanisms, the strongest direction of chemical bonding should be the one with the fastest crystal growth, which is favorable for the forming of a thin-film island in the initial stage. That is, following the nucleation and the ZnO film formation, the 30° rotation of the ZnO atomic arrangement that facilitates the first monolayer of the ZnO to adjust itself to the oxygen sublattice of the Al_2O_3 would stabilize the interface structures, which leads to the lattice mismatch of ZnO crystal and sapphire being diminished.

TABLE I. The atomic population and the charges for the ZnO and the surface O.

Atomic orbits	2s	2p	3s	3p	3d	4s	Charges
Zn		0.17[b]			9.93[b]	1.14[b]	0.70[b]
		0.32[a]			9.94[a]	0.64[a]	1.09[a]
O	1.97[b]	4.65[b]					−0.61[b]
	1.90[a]	5.13[a]					−1.03[a]
Al			0.51[b]	0.75[b]			1.75[b]
			0.46[a]	0.73[a]			1.81[a]
O*	1.89[b]	5.30[b]					−1.16[b]
	1.86[a]	5.40[a]					−1.29[a]

Note: O* is the surface O atoms bonded with the Zn:
[a] after adsorption.
[b] before adsorption.

After the surface adsorption of the ZnO, we discover that the ZnO adsorptive molecule has a certain impact on adjacent surface atomic structure. During the physical adsorption stage, as the ZnO molecule approaches the surface adsorption site, the surface Al at adjacent ZnO will move outside a distance of about 0.04±0.005 nm, and the interlayer distance of the first O-Al layer of the surface is about 0.06 nm, which is still less than the O-Al inter-layer distance of the α-Al_2O_3(0001) bulk (0.084 nm). Following the beginning of chemical adsorption, the surface Al continuously rises to form bonding with the O of the ZnO molecule. After bonding, the distance of the surface Al from the first O-layer of the surface is 0.08±0.005 nm, which is close to the Al-O interlayer distance in bulk, and the original surface Al-O relaxing will be slowly decreased, even eliminated finally. But the rising distance of the surface O atoms close to the Zn is small with less than 0.03 nm. There are hardly any changes in the interlayer distance of the surface atom far from the ZnO molecule.

C. Analysis on Mulliken populations

It can be seen from Table I that the O 2p orbits population and the negative charge of the ZnO after adsorption is increased. The population from the s orbits of the surface Al bonded with the ZnO is slightly reduced. It indicates that the positive charge of the surface Al is increased, a sign causing that part of the electrons from the s orbits of the surface Al have transferred into the O 2p of the ZnO molecule, thus causing the (Zn)O-Al bond to have a character of ionic bonding.

The population of the Zn 4s after adsorption obviously decreases, while that of the electrons of the surface O* 2p nearby the Zn atoms is increased. Both the negative charge of the O* 2p and the positive charge of the Zn also increase, which reveals that part of the electrons from the Zn 4s have transferred into the surface O* 2p after adsorption.

There are some kinds of electronic states within 0.17 of the occupied population in the p orbits of the Zn before adsorption that comes from the O 2p and partly hybridized with d orbit.[32,33] The electrons occupied population of the Zn p orbits after adsorption increase to 0.32, which indicates that the hybridization in 2p is further strengthened. We conclude that the hybridization comes from two aspects: one is the hybridization of the Zn 4s with the O 2p of the surface, the other the enhanced hybridization of the Zn 3d with the O 2p. It will be further discussed in the next sections. Therefore, the bonding of the Zn and the surface is not purely ionic bonding, but also has certain covalent characteristic whose details will be discussed in next section.

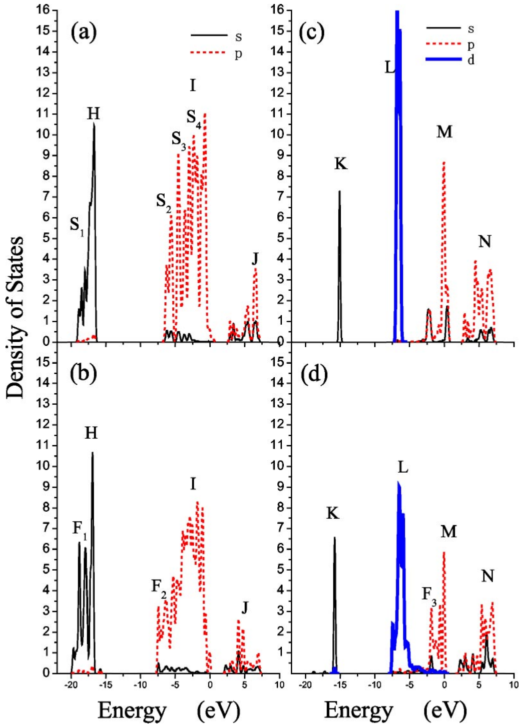

FIG. 5. (Color online) The PDOS of the surface Al-O atoms layer and the ZnO before and after the adsorption: (a) and (b) show the PDOS of the surface before and after adsorption, respectively. (c) and (d) show the PDOS of the ZnO before and after the adsorption, respectively.

D. Bonding and density of state

In order to further analyze the changes of electronic state before and after the adsorption and bonding of the ZnO on the α-Al_2O_3(0001), we calculate the PDOS of the ZnO by use of the software package. The PDOS of the Al-O layer at the α-Al_2O_3(0001) surface is divided into 3 groups. The peak of Group H is the bonding state of the surface O, which comes from the 2s and the 2sσ states formed by the O s and the Al s orbits in crystal field, as is shown in Fig. 5(a). The peak of Group I mainly comes from the 2pσ formed by the surface O and Al, and the 2pπ bonding orbits. The peak of Group J mainly comes from the 2pπ^* and 2pσ^* antibonding obits, as well as the surface state of the Al 3p. After the ZnO adsorption on the substrates, the changes in the PDOS of the surface Al-O layer are plotted in Fig. 5(b). A new DOS peak F_1 up to 6.2 e/eV appears at the left of Group H, which comes from the bonding peak formed by the Zn 4s of the

ZnO molecule. The peak of Group I is widened after the adsorption with its average peak obviously lowered, and moved to the left about 1 eV, which appears at the peak F_2 in low energy.

The surface O 2p obits overlapping the Zn 4s obits in the peak of Group I [Fig. 5(b)] produces a mixed state, implying that there is a hybridization from the 2p and the Zn 4s, which reduces the average DOS of the O 2p after adsorption, and results in an obvious reduction in the energy of bonding orbit p after adsorption. The original surface states S_1, S_2, S_3, and S_4 are redistributed and formed into a new surface electronic structure.

In view of the space position and energy of Zn adsorption ($S6 \rightarrow S7$, $S6 \rightarrow S5$), the hybridized orbits form the Zn 4s and the surface O 2p in the initial adsorption of the ZnO molecule tends to be sp^3. It reveals that the initial adsorption and the hybridized characteristic of the ZnO molecule on the α-$Al_2O_3(0001)$ surface would be help to form the Zinc Oxide crystal with tetrahedral coordination formed by the sp^3 hybridized orbit. As it has the wurtzite structure, the direction of each apex is parallel to the c-axis [0001]. This is why the ZnO film tends to grow toward the [0001] direction and to orient the (0001) of sapphire (0001). Accordingly, self-textured, the regular ZnO films are easily obtained.

The PDOS of the ZnO is divided into 4 groups of peaks shown in Fig. 5(c). The peak K mainly comes from the O 2s, the peak L is the electronic states of the Zn 3d, the peak M mainly comes from the bonding orbits of the O 2p, and the peak N is the orbits of corresponding antibonding. When the ZnO molecule is adsorbed [Fig. 5(d)], the energy distribution of the electronic states in the s orbits will be reduced about 0.4 eV and 0.8 electron/eV for the peak value. It can be seen from the figure that the s states are decreased, which reveals that there are electrons transferred from the Zn 4s into the surface for bonding. Electrons from the surface Al 3s move to the O 2p of the ZnO molecule for bonding, which causes the O 2p bonding peak of the ZnO molecule after adsorption to become widened and move to the left. It is obviously shown at bonding peak F_3 [Fig. 5(d)]. The peak L(Zn 3d) also widens, obviously, and further splits after adsorption, which causes quite few of the O 2p electron states to be mixed in, and the maximum peak value reduce about 7.1 electron/eV due to the total energy reduction of the d orbits resulting in ligand field stabilization energy (LFSE).

A comparative analysis of the peaks L and I in Fig. 5(d) and 5(b) manifests that the electronic states of the Zn 3d will overlap more with the O 2p of the Al_2O_3 substrates ($-7.8-0.0$ eV) and produce strong mixed states between $-7.8--4.5$ eV. That is to say, it is possible for the energy level of part of the electrons at the Zn 3d close to part of the O 2p to form a hybridized bond with the surface O.[34] Researches in Refs. 35–37 deduce that it is possible for the Zn 3d of ZnO crystal to hybridize with the O 2p according to its point group coordinate, and the formed hybrid band s-d has a very important function on bonding. We find that the splitting of the Zn 3d strongly interacts with the O 2p electrons at the Zn adsorbed sites in the surface, thus leading to obvious reduction of energy in Zn 3d after adsorption. Compared with the gaseous ZnO molecule before adsorption, the higher-energy electronic states are weakened, which reduces the system energy after adsorption.

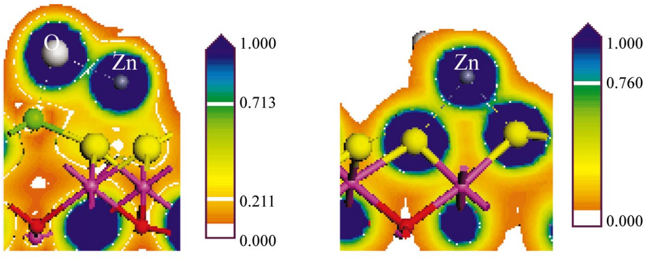

(a) (b)

FIG. 6. (Color) The ELF for the ZnO and the surface bonding: (a) the slice vertical to the surface along $[\bar{1}2\bar{1}0]$ direction passing through the ZnO is for the ELF of the Zn-O-Al bond. (b) the slice vertical to $[01\bar{1}0]$ direction and the surface passing through the Zn is for the ELF of the Zn-O(substrate) bond [see Fig. 4 B-④].

E. Electron localization function

The electron localization function (ELF) is used in observing atomic shell structure and core, bonding and lone electorn pairs, and bonding electronic regions in solid, which reveals the chemical bonding characteristics and types, such as metallic, ionic, covalent, and dangling bonding.[38–41]

Figure 6(a) shows the ELF distribution value of the Zn-O and the (Zn) O-Al (substrate) bond after the chemical adsorption. Figure 6(b) illustrates the ELF of the Zn-O (with two substrate O* atoms) formed at the adsorption sites of the Zn. The different colors in the figure represent the relative electronic density. In Fig. 6(a), the ELF value of the (Zn)O-Al chemical bond is 0.211, where the electrons mainly gather around the O atom, and have obvious character of ionic bonding. The ELF value at the ZnO chemical bond is 0.713, where the character of ionic bonding is weakened and some covalent characters appear. In Fig. 6(b), the ELF between the two chemical bonds of the Zn and the two oxygen atoms of the surface is greater than 0.760, with the shorter one of ELF 0.870 showing obviously more of the character of covalent bonding.

IV. CONCLUSION

The calculation on the α-$Al_2O_3(0001)$ surface relaxing is well conformed with previous studies. Through a comparison of the PDOS of the outermost surface Al and O layer before and after relaxing, it has been further described that the distribution of the α-$Al_2O_3(0001)$ surface states is obviously shown in O-surface states, which mainly comes from the changes of the surface O 2p electronic states. The shrinkage of the surface Al-O bonds and the existence of the s-p hybridization result in even lower surface energy ($1.60\ J/m^2$), but still have the distinct character of ionic bonding.

An analysis of the dynamic process of model A and B shows the 4 stages in the adsorption process of the ZnO on the α-$Al_2O_3(0001)$ surface: physical adsorption and migration, chemical adsorption of (Zn)O-Al, chemical adsorption of Zn-O (substrate), and bonding at the optimal adsorption positions. The bonding energy of the ZnO molecule at the α-$Al_2O_3(0001)$ surface is greater than 4.4 ± 0.4 eV. It is found that the bond of the ZnO molecule has a 30° deflexion angle from the adjacent Al-O bond of the surface after adsorption, and the stabilized chemical adsorption sites S5 and S7 are about 30° away from the O hexagonal symmetry of the sapphire(0001) substrate, which reduce and even eliminate the relaxing at the surface Al-O layer before adsorption. These calculation results are well in agreement with related experimental researches.[2–6] After the adsorption of the ZnO on the surface, part of electrons at the Zn 4s obits obviously transfer into the α-Al_2O_3(0001) surface. The chemical (Zn)O-Al(substrate) bond has the character of ionic bonding, while the Zn-O (substrate) bond obviously has the covalent character. The covalent character of the Zn-O (substrate) bond mainly comes from the hybridization of the Zn 4s and the surface O 2p, and partly from the hybridization of the Zn 3d and the O 2p orbits. In addition, in view of the atomic population, the PDOS before and after the adsorption, adsorption energy, and adsorption sites, it is favorable for the sp^3 hybridization of the Zn 4s with the O 2p of the surface, for forming the tetrahedral coordinate and for shaping the wurtzite structure of the ZnO thin films.

ACKNOWLEDGMENTS

This research work has been supported by the State Key Development Program for Basic Research of China (Grant No. 51310Z03) and the Application and Basic Research of Sichuan Province under Grant No. 02GY-006. We wish to acknowledge the support from the Software Key Laboratory of Sichuan Normal University and the Center of Computer Simulation, China Academy of Engineering Physics. The authors would like to thank Professor Z. Z. Yun, Y. Zhang, and W. D. Xue for their numerous and useful suggestions and help.

---

[1] Z. Marian, K. Alexey, G. Bernard, M. Guillaume, and K. Mikhail, Phys. Rev. B **65**, 161205 (2002).

[2] C. Yefan, D. M. Bagnall, Hang-jun Koh, Ki-tae Park, Kenji Hiraga, Ziqiang Zhu, and Takafumi Yao, J. Appl. Phys. **84**, 3912 (1998).

[3] P. Fons, K. Iwata, S. Niki, A. Yamada, and K. Matsubara, J. Cryst. Growth **201/202**, 627 (1999).

[4] E. Millon, O. Albert, J. C. Loulergue, J. Etchepare, D. Hulin, W. seiler, and J. Perierère, J. Appl. Phys. **88**, 6937 (2000).

[5] I. Ohkubo, A. Ohtomo, T. Ohnishi, Y. Mastumoto, H. Koinuma, M. Kawasaki, Surf. Sci. **443**, L1043 (1999).

[6] I. Ohkubo, Y. Matsumoto, A. Ohtomo, T. Ohnishi, A. Tsukazaki, M. Lippmaa, H. Koinuma, and M. Kawasaki, Appl. Surf. Sci. **159–160**, 514 (2000).

[7] B. Dam and B. S. Pümpin, J. Mater. Sci.: Mater. Electron. **9**, 217 (1998).

[8] N. M. Harrison, Comput. Phys. Commun. **137**, 59 (2001).

[9] I. Manassidis, A. D. Vita, and M. J. Gillan, Surf. Sci. **285**, L517 (1993).

[10] R. D. Felice and J. E. Northrup, Phys. Rev. B **60**, R16287 (1999).

[11] R. Baxter, P. Reinhardt, N. Lopez, F. Illas, Surf. Sci. **445**, 448 (2000).

[12] A. Wander, B. Searle, N. M. Harrison, Surf. Sci. **458**, 25 (2000).

[13] J. R. B. Gomes, I. de P. R. Moreira, P. Reinhardt, A. Wander, B. G. Searle, N. M. Harrison, and F. Illas, Chem. Phys. Lett. **341**, 412 (2001).

[14] T. J. Godin and P. J. LáFemina, Phys. Rev. B **49**, 7691 (1994).

[15] V. E. Puchin, J. D. Gale, A. L. Shluger, E. A. Kotomin, J. Günster, M. Brause, and V. Kempteret, Surf. Sci. **370**, 190 (1997).

[16] X. G. Wang, A. Chaka, and M. Scheffler, Phys. Rev. Lett. **84**, 3650 (2000).

[17] J. P. Perdew, J. A. Chevary, S. H. Vosko, K. A. Jackson, M. R. Pederson, D. J. Singh, and F. Carlos, Phys. Rev. B **46**, 6671 (1992).

[18] D. Vanderbilt, Phys. Rev. B **41**, 7892 (1990).

[19] M. C. Payne, M. P. Teter, D. C. Allan, T. A. Arias, and J. D. Joannopoulos, Rev. Mod. Phys. **64**, 1045 (1992).

[20] L. J. Clarke, I. Štich, and M. C. Payne, Comput. Phys. Commun. **72**, 14 (1992).

[21] M. J. S. Spencer, A. Hung, I. K. Snook, and Y. Irene, Surf. Sci. **513**, 389 (2002).

[22] M. Yi and M. L. Li, Chem. J. Chinese Universities **22**, 81 (2001).

[23] T. H. Fischer and J. Almlof, J. Phys. Chem. **96**, 9768 (1992).

[24] W. C. Robert, A. J. Melvin, and B. H. William, *CRC Handbook of Chemistry and Physics* (CRC Press, Inc., Florida, 1993).

[25] M. Dolg, U. Wedig, and H. Stoll, J. Chem. Phys. **86**, 2123 (1987).

[26] D. S. Portal, E. Artacho, and J. M. Soler, Solid State Commun. **95**, 685 (1995).

[27] R. S. Mulliken, J. Chem. Phys. **23**, 1833 (1955).

[28] R. W. G. Wyckoff, *Crystal Structures*, 2nd ed. (Interscience, New York, 1964).

[29] J. Toofan and P. R. Watson, Surf. Sci. **401**, 162 (1998).

[30] X. G. Wang, A. Chaka, and M. Scheffler, Phys. Rev. Lett. **84**, 3650 (2000).

[31] D. Siegel, L. G. Hector, Jr., and J. B. Adams, Phys. Rev. B **65**, 085415 (2002).

[32] P. Schröer, P. Krüger, and J. Pollmann, Phys. Rev. B **47**, 6971 (1993).

[33] D. Vogel, P. Kruger, and J. Pollmann, Phys. Rev. B **52**, R14316 (1995).

[34] C. D. Gelatt, A. R. Williams, and V. L. Moruzzi, Phys. Rev. B **27**, 2005 (1983).

[35] D. Vogel, P. Kruger, and J. Pollmann, Phys. Rev. B **52**, R14316 (1995).

[36] F. Norifumi, N. Tokihiro, G. Seiki, Xu Jifang, and I. Taichiro, J. Cryst. Growth **130**, 269 (1993).

[37] S. V. Prasad, S. D. Walck, and J. S. Zabinski, Thin Solid Films. **360**, 107–117 (2000).

[38] V. Tsirelson and A. Stash, Chem. Phys. Lett. **351**, 142 (2002).

[39] D. L. Santis and R. Resta, Solid State Commun. **111**, 583 (1999).

[40] L. D. Santis and R. Resta, Surf. Sci. **450**, 126 (2000).

[41] L. G. Hector, Jr., S. M. Opalka, G. A. Nitowski, L. Wieserman, D. J. Siegel, H. Yu, and J. B. Adams, Surf. Sci. **494**, 1 (2001).